INELASTIC SEISMIC RESPONSE ANALYSES OF REINFORCED CONCRETE BRIDGE PIERS WITH THREE-DIMENSIONAL FE ANALYSIS METHOD

Guangfeng Zhang[1], Shigeki Unjoh[2]

Abstract

This paper aims to provide an analysis method for simulating the seismic behavior of a RC pier under multi-directional seismic excitation. Three-dimensional elasto-plastic finite element method was adopted with a purpose to make it possible to consider the failure mode of flexure-shear failure at the termination location of the main rebar. Two RC pier specimens, in which one failed in flexure failure at the base of the pier and the other failed in flexure-shear failure at the main rebar termination location, were analyzed and the validity of the analysis method was discussed. Discussion results show that the analyses provided a successful identification of the failure mode and a good simulation of the seismic behavior before the effect of concrete cover spalling over the responses become dominant.

Introduction

A number of highway bridges were destroyed or damaged in the 1995 Hyogo-ken Nanbu Earthquake occurred in the Kobe area, Japan. A typical damage pattern of reinforced concrete (RC) piers confirmed in this earthquake was flexure-shear failure at the main rebar termination location, at which main rebars were cut-off with a certain ratio based on design moment for saving the cost. Figure 1 shows RC piers collapsed or damaged with flexure-shear failure in the 1995 Hyogo-ken Nanbu Earthquake. In Japan, Termination of main rebar was generally adopted in design before 1980.

Fig. 1 Flexure-shear Failure of RC Piers in the 1995 Hyogo-ken Nanbu Earthquake

The essential reason of the flexure-shear failure was premature termination of the

[1] Researcher, Bridge and Structural Technology Research Group, Public Works Research Institute, Japan
[2] Chief Researcher, Bridge and Structural Technology Research Group, Public Works Research Institute, Japan

main rebar. This type of failure initiates generally with flexural failure at the main rebar termination location and then develops in many case to brittle failure such as shear failure. Strength and ductility of a pier will become lower than design if it failed in the flexure-shear failure at the main rebar termination location prior to the designed flexure failure of the base of the pier. When evaluate the seismic vulnerability of a RC pier with termination of the main rebar at midheight, it is necessary to make it possible to take the effects of the termination of the main rebar into account in the computation.

This research aims to provide an analysis method for simulating the seismic behavior of a RC pier with consideration of the effects of the main rebar termination. Three-dimensional elasto-plastic finite element method was adopted because it is possible to model the main rebars and hoop rebars with an arrangement according to the real structure. At the same time, it is easy to take into account of the nonlinear behavior of materials such as concrete cracking, concrete crushing and rebar yielding. Test results of two RC pier specimens, in which, one without main rebar termination failed in flexure failure at the base of the pier and the other with main rebar termination failed in flexure-shear failure at the main rebar termination location, were employed to investigate the validity of the analysis method. Discussions of the investigation were conducted based on comparisons of the natural period of the test system, response displacement and damage progression of the piers. Commercial FEM package DIANA (DIANA 7.2) was used in this research.

Overview of Tests

Design of Specimens

Two RC pier specimens tested by Sakai et al. (Sakai et al., 2007) were employed to investigate the validity of the proposed analysis method. The two specimens were designed with the 1970's seismic design code for the purpose to simulate the damages of RC bridges damaged in the 1995 Hyogo-ken Nanbu Earthquake, which were constructed with a seismic design code of 1970's. One specimen was designed as a flexure failure type at the base of the pier (hereafter, designated as specimen F) and the other was designed as a flexure-shear failure type at main rebar termination location (hereafter, designated as specimen FS). Figure 2 shows the details of the two specimens. Both of the two specimens are circular cross section with a diameter of 600 mm and a column height of 2,000 mm. Specimen F was reinforced longitudinally with 80 of 10-mm deformed rebars without termination along the height of the pier. Specimen FS was reinforced longitudinally with 100 of 10-mm deformed rebars at the base and the rebars were cut off two times at heights of 630 mm and 1,300 mm. Rebar with a diameter of 3-mm was used as hoop rebar for both of the two specimens.

Table 1 shows the material properties of concretes and rebars obtained from tests.

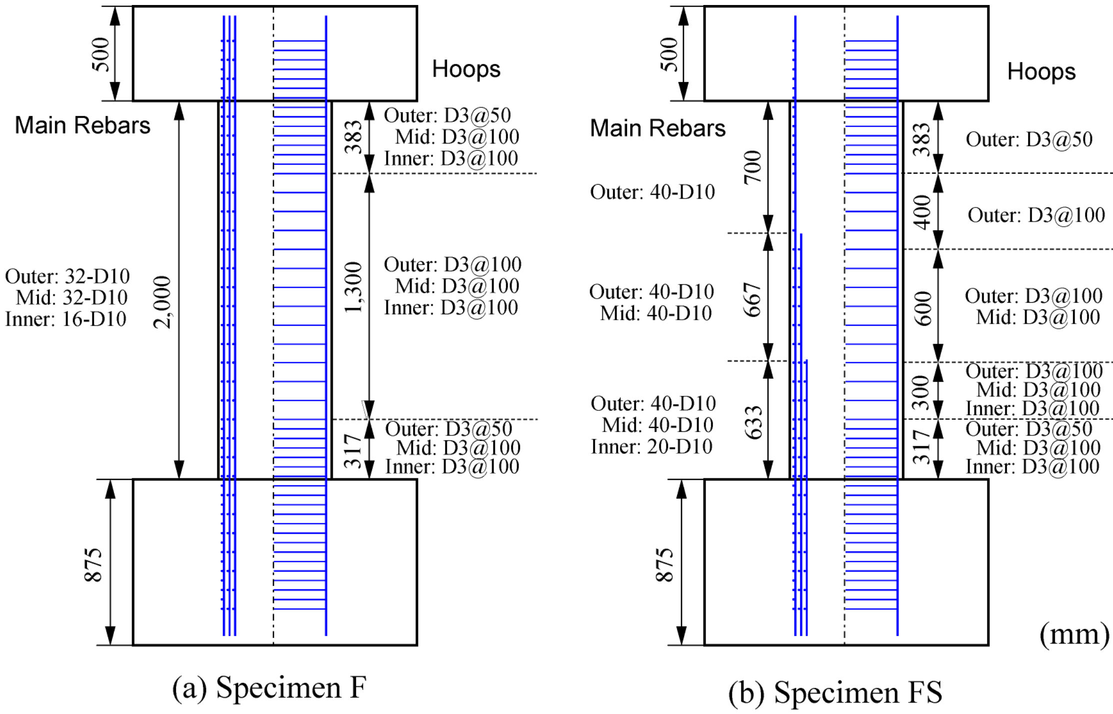

Figure 2 Details of Specimens

Table 1 Material Properties

	Compressive Strength (N/mm^2)	Yield Strength (N/mm^2)	Young's Modulus (N/mm^2)
Concrete (Specimen F)	27.9	-	2.88×10^4
Concrete (Specimen FS)	28.8	-	2.65×10^4
Main Rebar (SD295A, Specimen F)	-	351.4	1.78×10^5
Main Rebar (SD345, Specimen FS)	-	374.2	1.80×10^5
Hoop Rebar	-	280.4	2.13×10^5

Setup of Tests

The two specimens were tested dynamically with three-directional ground motions input under a large-scale three-dimensional shake table (Sakai et al., 2007). Figure 3 shows the details of the setup. Girders and top masses were installed with the support of the safety frames for modeling the superstructure. Total weight of the girders and top masses was set as 260 kN, which provided an axial stress of 1.04 N/mm^2 in the column. The height of the center of gravity was 2,500 mm in the longitudinal direction (X-direction) and 3,650 mm in the transverse direction (Y-direction).

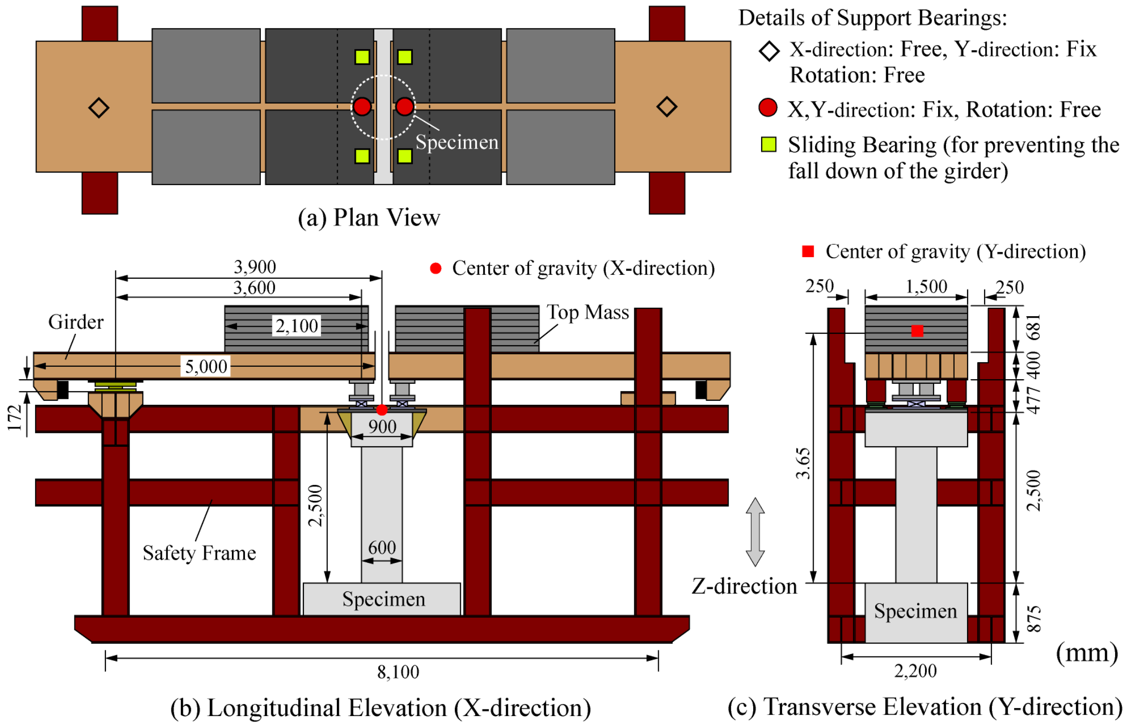

Figure 3 Setup of Tests

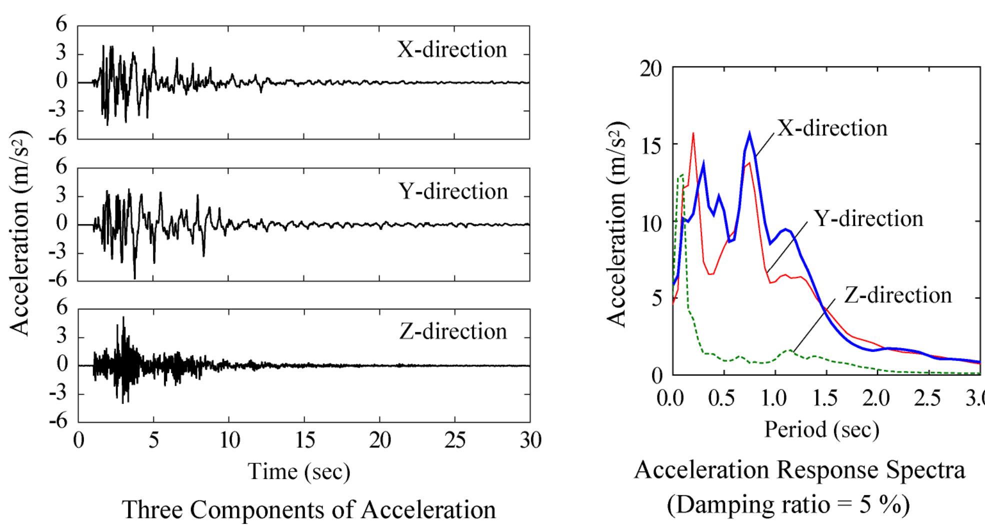

Figure 4 Input Ground Motions

Input Ground Motions

The ground motions recorded at the Takatori Station during the 1995 Hyogo-ken Nanbu Earthquake were employed in the tests. The amplitude was scaled down to 80% taking into account of the capacity of the specimens (Sakai et al., 2007). Figure 4 shows the three components and response spectra.

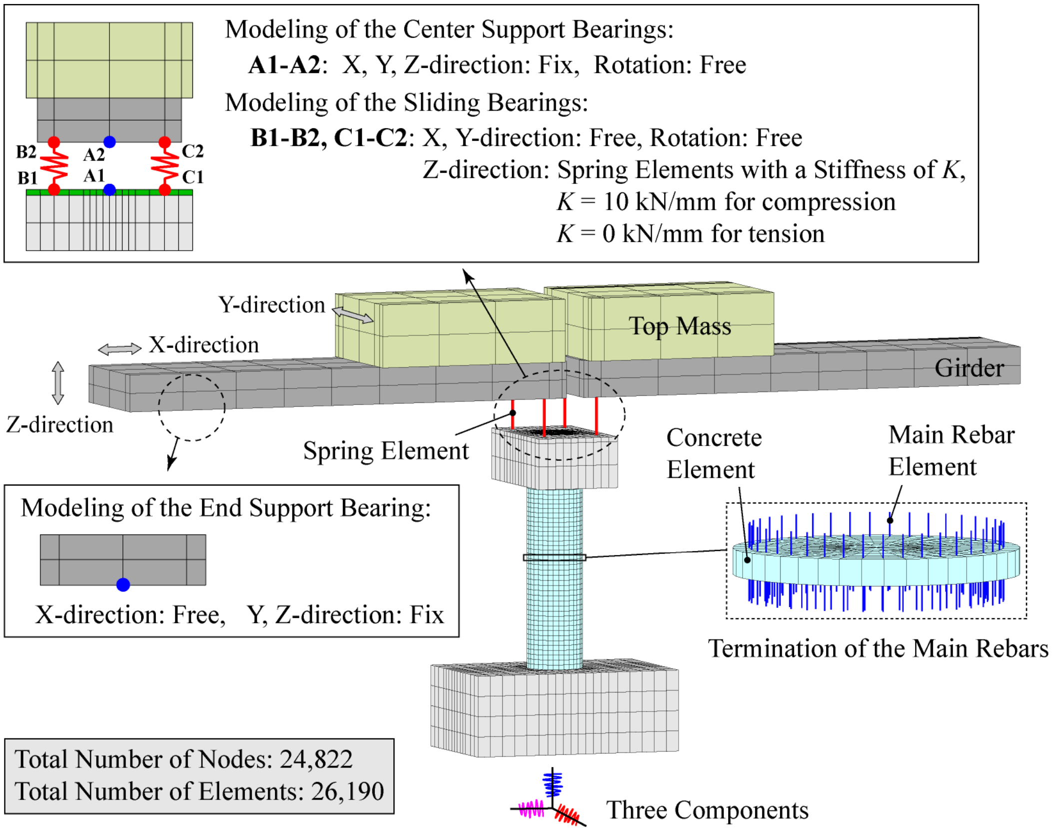

Figure 5 FE Model of Specimen FS

<u>Overview of Analyses</u>

FE Modeling of Specimens

Figure 5 shows FE model of specimen FS as an example. Concrete was modeled using eight-node solid element. Main rebar was modeled using truss element assuming perfect bonding between rebar and concrete. Termination of the main rebar was considered by cutting off the truss elements with the same numbers at a height same as the specimen. Hoop rebar was modeled using embedded reinforcement element, which is a type of element for modeling the reinforcement by embedded in the concrete element (DIANA 7.2). The embedded reinforcement elements were arranged coinciding with the arrangement of the hoop rebars in the specimens.

Support bearing was modeled by providing a similar restraint condition by means of boundary condition or spring element. End support bearings were modeled by constraining the freedom of the nodes located at the center of the bearings in Y, Z-direction. The freedom in X-direction and rotation were kept in free. Central support bearing above the pier was modeled by fixing the relative displacement between nodes A1 and A2 in three directions. Rotation between the two nodes was allowed. Sliding bearings installed on the side of the central support bearing were modeled using spring elements. Working direction of the spring element was Z-direction. Stiffness *K* was assumed as 10 kN/mm for compression and 0 kN/mm for tension. This means that the spring element works just when it is compressed in the working direction (Z-direction). Here, the value of stiffness *K* was determined by sensitivity analysis on the natural period of the test system in transverse direction. It was concluded that K = 10 kN/mm provides a good simulation as shown in Table 2. No constraint was applied in the two horizontal directions between nodes B1-B2 and nodes C1-C2 ignoring the horizontal friction of the sliding bearings.

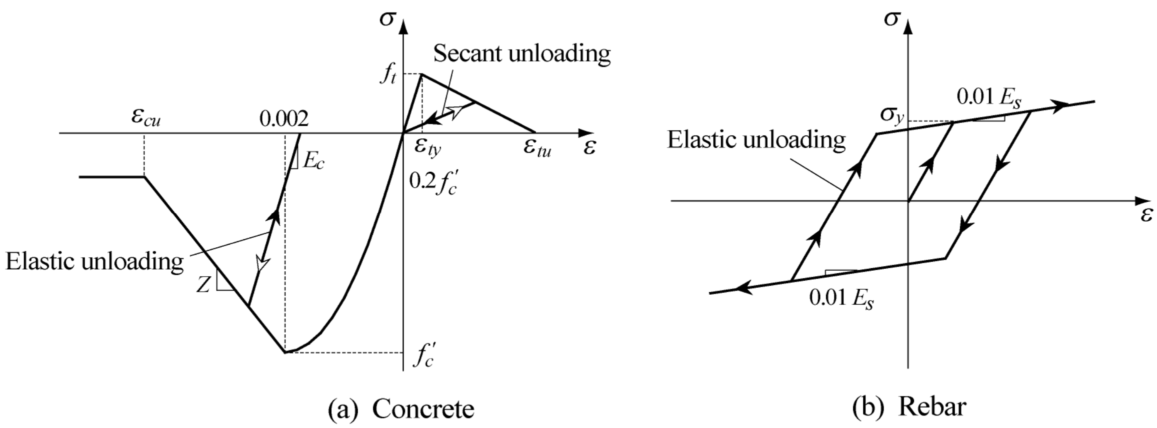

Figure 6 Constitutive Models

Material Models

Figure 6(a) shows the constitutive model for concrete. Park model (Kent and Park, 1971) was employed in compression. The ascending branch before the maximum strength is a second-order parabola curve defined with equation (1). The descending branch in the post peak region is described by a straight line with a slope of *Z* determined by equation (2). The Mohr-Coulomb yield criterion with associated plastic flow was used to define the yielding state of concrete, in which friction angle was taken as 30 degree (DIANA 7.2).

$$\sigma = f'_c\left[\frac{2\varepsilon}{0.002}-\left(\frac{\varepsilon}{0.002}\right)^2\right] \tag{1}$$

$$z = \frac{0.5}{\left(\dfrac{3+0.002f'_c}{f'_c-1000}\right)-0.002} \qquad \text{(Unit: } psi\text{)} \tag{2}$$

$$\varepsilon_{tu} = \frac{2G_f}{f_t h_{eq}} \tag{3}$$

$$G_f = 10(d_{\max})^{1/3} \cdot f'_c{}^{1/3} \tag{4}$$

A linear tension-softening model was employed in tension. Ultimate tensile strain ε_{tu} was determined by equation (3) (JSCE, 2002). Here, G_f is the tensile fracture energy of concrete estimated by equation (4) (DIANA 7.2); f_t is the tensile strength of concrete; h_{eq} is the equivalent length of a concrete element and d_{max} is the maximum size of the aggregate. A smeared crack model was applied to take into account of the concrete cracking. According to this model, a crack is considered as opened orthogonal to the direction of the principal tensile stress once the principal tensile stress exceeds the tensile strength of the concrete. Shear modulus of an element after cracked was assumed to be 5% of the initial shear modulus *G* of the concrete.

A bilinear kinematic hardening model as shown in Fig. 6(b) was used for rebar. Plastic hardening coefficient was assumed to be 1% of the Young's modulus. The von Mises yield criterion was used to define the yielding state of rebar.

Input Ground Motions

Three components of response accelerations measured at the top surface of the shake table were applied as input ground motions in the analyses. The components were input on the nodes of the bottom surface of the footing with a time step of 0.02 second. Damping ratio was taken as 0% in this research.

Results of the Analysis and Discussions

Each of the two analyses was conducted with an excitation time of 5.0 seconds. Natural period of the test system, response displacement and damage progression of the pier were compared to investigate the validity of the analysis results. Here, damage progression for the two specimens obtained in the tests were shown in Figs. 7 and 8 for references. Specimen F failed in flexure at the base of the pier. Spalling of the concrete cover and buckling of the main rebar extended to about 400 mm height after test. Specimen FS failed in flexure-shear at the main rebar termination location. Figure 8 shows that flexural failure occurred at the main rebar termination location at 2.8 seconds and a shear crack developed from the main rebar termination location at 2.9 seconds.

Natural Periods

Table 2 shows the comparison of natural periods of the test system. Natural periods in the transverse direction were evaluated with a good accuracy because they were calibrated in the previous sensitivity analyses. Natural periods in the longitudinal direction were evaluated as 82.9% and 83.5% of the test results for specimens F and FS, respectively. This implies that the test system in the longitudinal direction was modeled with a higher stiffness in the analysis. The reason can be attributed to the modeling method of the central support bearing (referring to Fig. 3). Fully fixing the relative displacement between nodes A1 and A2 in the three directions resulted in a higher constraint effects than that of the bearing.

(a) 3.1 seconds (b) 3.6 seconds (c) After Test

Figure 7 Damage Progression of Specimen F

(a) 2.8 seconds (b) 2.9 seconds (c) 3.0 seconds (d) 3.1 seconds (e) 3.7 seconds (f) 4.4 seconds

Figure 8 Damage Progression of Specimen FS

Table 2 Comparison of Natural Periods

	Longitudinal Direction			Transverse Direction		
	Test (sec)	Ana. (sec)	Ana. / Test (%)	Test (sec)	Ana. (sec)	Ana. / Test (%)
Specimen F	0.251	0.208	82.9	0.394	0.395	100.3
Specimen FS	0.266	0.222	83.5	0.385	0.405	105.2

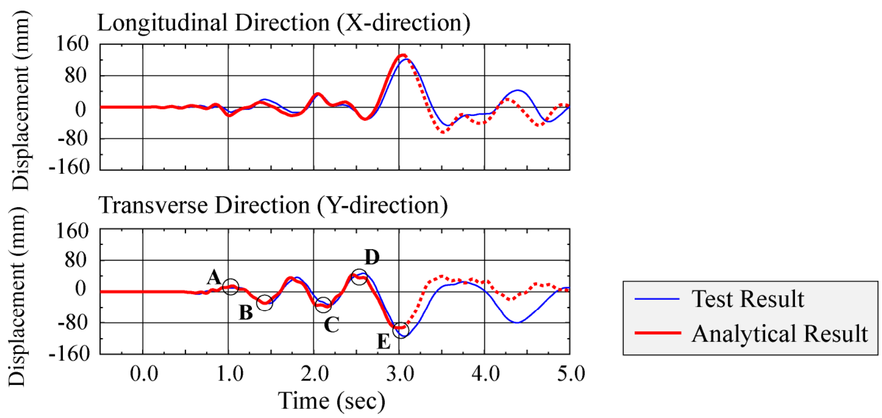

(a) Specimen F

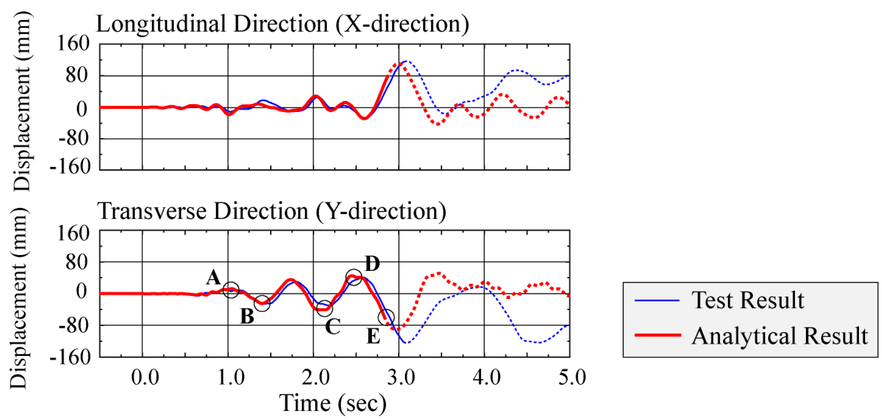

(b) Specimen FS

Figure 9 Comparison of Response Displacements at the top of the Pier

Response Displacements

Figure 9 shows the comparison of response displacements at the top of the pier. It is noticed that analysis for each of the two specimens provides an approximate simulation until a peak around 3.0 seconds but the analytical results after that are rather different with the test ones in terms not only of the period but also of the amplitude. This is mainly attributed to the reason that influences of the concrete cover spalling and the main rebar buckling occurred after that were not accounted enough in the analysis. Although nonlinear behavior of the materials was considered, no special model was employed to take into account of the damages such as concrete cover spalling off and main rebar buckling. These failures involve large deformation and discontinuity.

Time history of the responses after 3.1 seconds for specimen F and 2.8 seconds for specimen FS were plotted as dash line to indicate that the responses were the ones obtained without enough consideration of the spalling off of the concrete cover. Here, excitation times of 3.1 and 2.8 seconds were the times at which spalling of the concrete cover was confirmed in the test of specimens F and FS, respectively, as shown in Figs. 6 (a) and 7 (a).

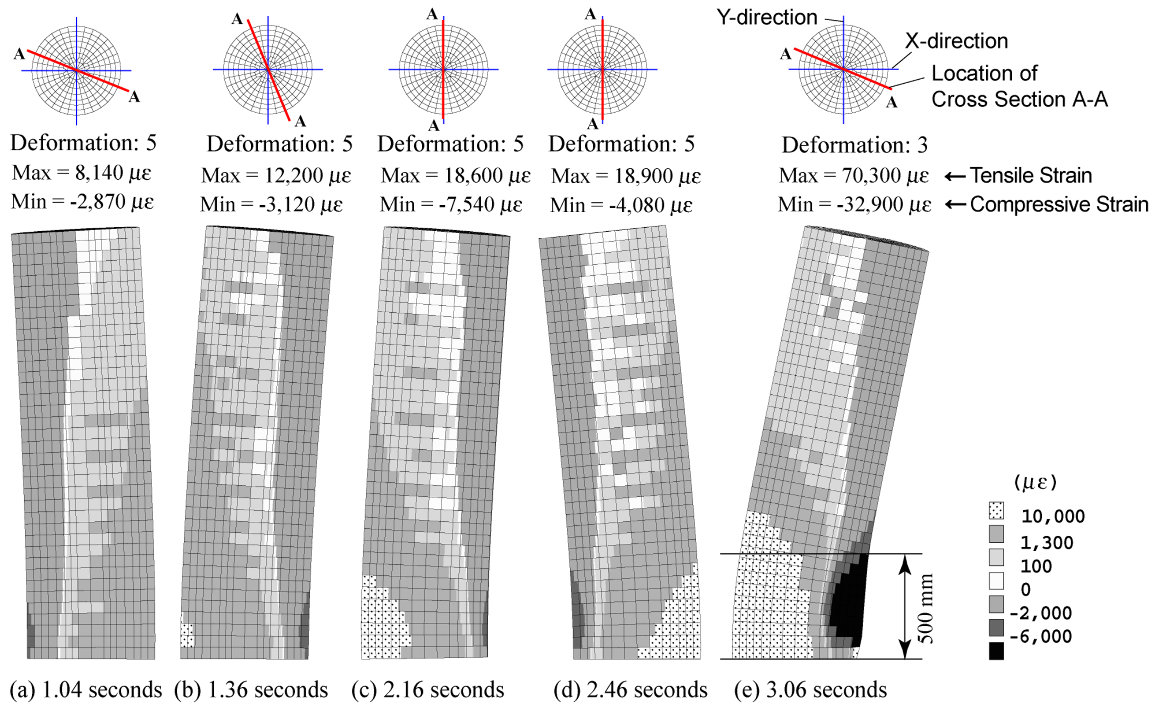

Figure 10 Concrete Strain Distribution of Specimen F in Z-direction (Section A-A)

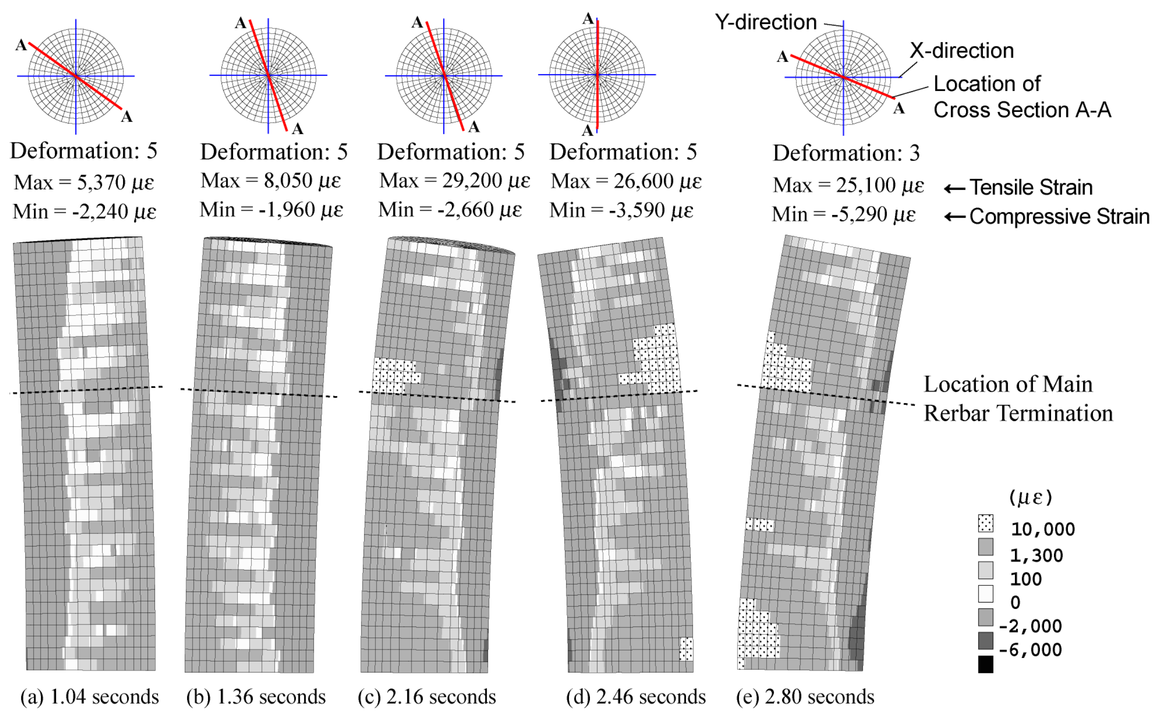

Figure 11 Concrete Strain Distribution of Specimen FS in Z-direction (Section A-A)

Damage Progression

Damage progression obtained from the analysis was expressed by concrete strain distribution along the height (Z-direction) of the pier. Figures 10 and 11 show the concrete strain distributions in a cross section A-A at the peaks of A to E shown in Fig. 9. Cross section A-A is a section along a line connecting the maximum tensile strain point and maximum compressive strain point. Strain levels -6,000, 100 and 1,300 $\mu\varepsilon$ are the approximate values of the strains ε_{cu} , ε_{ty} and ε_{tu} , as shown in Fig. 6. A region with compressive strain beyonds -6,000 $\mu\varepsilon$ or tensile strain beyonds 1,300 $\mu\varepsilon$ is considered as a compression failure region or an opened crack.

Figure 10(a) shows that cracked region extended over half height of the pier at 1.04 seconds. The outermost elements at the base of the pier, which have a thickness approximately same as that of the concrete cover, were compressed over 2,000 $\mu\varepsilon$. This means that the concrete in this region has begun to soften. A crack over 10,000 $\mu\varepsilon$ tensile strain appeared at 1.36 seconds. Cracking and softening extended at the base of the pier at times of 2.16 and 2.46 seconds. Figure 10(e) shows that the region with compressive strain over 6,000 $\mu\varepsilon$ extended to about 500 mm height at 3.06 seconds. It is noticed that this agrees approximately with the height of the concrete cover spalled region as shown in Fig 7(c).

Figures 11(a) and (b) shows that flexural cracks occurred along the whole height of the pier at 1.04 and 1.36 seconds. A region with over 10,000 $\mu\varepsilon$ tensile strain and over -2,000 $\mu\varepsilon$ compressive strain occurred at the main rebar termination location at 2.16 seconds and extended obviously at 2.46 seconds, as shown in Figs. 10(c) and (d). This means that flexural failure occurred at the main rebar termination location. At 2.8 seconds shown in Fig. 11(e), cracking and softening were also confirmed at the base of the pier as well as the main rebar termination location. This implies that the failure mode have shifted from the flexure failure at the main rebar termination location to the flexure failure of the base of the pier. The analysis evaluated a flexure failure at the base of the pier finally. Comparing to Fig.8(a), it can be said that flexural failure at the main rebar termination location at 2.8 seconds was approximately simulated by the analysis. However, the analysis can not provide a simulation of the shear failure initiated from the main rebar termination location.

Comparison of Fig. 10 and Fig. 11 shows that failure mode of the two specimens were identified successfully by the analysis.

Conclusions

An analysis method for simulating the seismic behavior of a RC pier under multi-directional seismic excitation was proposed based on three-dimensional FEM in this paper. Two RC pier specimens, in which one without main rebar termination failed in flexure failure at the base of the pier in test and the other with main rebar termination failed in flexure-shear failure at the main rebar termination location, were analyzed and the validity of the analysis method was confirmed by comparing the natural period of the test system, response displacement and damage progression of the piers.

Discussion results show that the analyses provided a successful identification of the failure mode and a good simulation of the seismic behavior before the effect of concrete cover spalling over the responses become dominant. However, the final failure stage involving concrete cover spalling off and shear failure initiated from the main rebar termination location can not be simulated by the current method. This becomes an issue in the next research stage.

References

Kent, D. C., and Park, R. (1971). “Flexural members with confined concrete”, *J. Struct. Div. ASCE*, 97(7), pp. 1969-1990, 1971.

Nonlinear Analysis User’s Manual (7.2), TNO Building and Construction Research.

Sakai, J., Unjoh, S. and Ukon, H. (2007). “Shake Table Test of Bridge Column Models Damaged during 1995 Hyogo-ken Nanbu Earthquake”, *Journal of Japan Association for Earthquake Engineering*, Vol.29, 2007.

Standard Specifications for Concrete Structures-2002, Structural Performance Verification, *JSCE*, 2002.